

Conf. 9109302-1

TWO- AND THREE-DIMENSIONAL FLOW SIMULATIONS OF INGOT GROWTH IN AN EBEAM FURNACE^{1,2}

P. R. Schunk, R. W. Fisher, and F. J. Zanner
Sandia National Laboratories
Albuquerque, New Mexico

SAND--91-2288C
DE92 002349

ABSTRACT

Electron-Beam (EBeam) melting furnaces are routinely used to minimize the occurrence of second-phase particles in the processing of segregation-sensitive alloys. As one part of the process, a circulating electron beam impinges the surface of a crucible melt pool to help control the shape of the solidification front below. By modeling melt pool hydrodynamics, heat transfer, and the shape of solidification boundaries, we plan to optimize the dwell pattern of the beam so that the material solidifies with a composition as spatially homogeneous as possible.

Both two- and three-dimensional models are being pursued with FIDAP 5.02, the former serving as a test bed for various degrees of model sophistication. A heat flux distribution is specified on the top of the domain to simulate the EBeam dwell pattern. In two dimensions it is found that an inertially-driven recirculation in the melt pool interacts with a counter-rotating buoyancy-driven recirculation, and that both recirculations are influenced heavily by surface tension gradients on the melt-pool surface. In three dimensions the inertial cell decays quickly with distance from the position of the inlet stream, causing the fluid to precess the crucible. Ingot macrosegregation patterns for a U-6 wt. % Nb alloy are calculated with the Flemings-Mehrabian equation of solute redistribution; the sensitivity of these patterns to EBeam dwell pattern is explored.

¹This work was performed at Sandia National Laboratories, which is operated for the U.S. Department of Energy, under contract number DE-AC04-76DP00789. Funding for this work was provided by Martin Marietta Y12

² To be published in the Proceedings of the 1991 Vacuum Metallurgy Conference on The Melting and Processing of Specialty Materials, 9-11 September, Pittsburgh, PA.

MASTER

DISTRIBUTION OF THIS DOCUMENT IS UNLIMITED

4P2

1 INTRODUCTION

EBeam furnaces are routinely used to minimize the occurrence of second-phase particles in the processing of segregation-sensitive alloys. This presentation describes the first phase of a joint effort between Sandia National Laboratories and Martin Marietta Y12 to develop a process to recycle refractory alloy machining chips/scrap back into the production stream. Sandia's role is to provide modeling support in the design of a prototype furnace.

Sandia's EBeam furnace was designed as a multi-application research furnace with consideration of uranium machining scrap recycling as a primary program requirement. The complete melting process is shown in Fig. 1. The first part of the process is a premelting step, or hearth melting, whereby scrap metal chips are placed in a hearth and melted with a circulating electron beam. The refined molten metal then spills into a melt pool in the cylindrical crucible below. There the molten metal undergoes controlled solidification, with heat being drawn off by a thermal jacket around the crucible. A second electron beam circulates on the surface of a melt pool to help control the shape of the solidification front below. Solidified material is ultimately drawn off as a cylindrical ingot.

Because of harsh conditions in the furnace, little can be done experimentally to understand how the dwell pattern of an electron beam affects the melt pool hydrodynamics. By modelling melt pool hydrodynamics, heat transfer, and the shape of solidification boundaries, we plan to optimize the dwell pattern of the beam so that the material solidifies with a composition as spatially homogeneous as possible.

2. ANALYSIS

So far the modelling effort is focused downstream of the hearth melting step; the domain extends from the point at which refined molten metal spills into the crucible to the bottom of the crucible where the solid ingot is drawn off. The crucible shape is axisymmetric, but the transport fields within are three-dimensional, insofar as the feed stream is off-axis. For practical reasons molten metal is always poured near the crucible wall to avoid EBeam shading. Both two- and three-dimensional models are being pursued with the finite element computer code FIDAP 5.02, the former serving as a test bed for various degrees of model sophistication.

The theory thus far is adequately described by the Navier-Stokes equations and the energy equation for incompressible Newtonian flow. Constitutive equations for temperature-dependent thermophysical properties are employed where appropriate. A special boundary condition is applied to the heat transport field at the crucible wall to account for ingot shrinkage during solidification. A heat flux distribution is specified on the top of the domain to simulate the E-Beam dwell pattern.

The two-dimensional meshes we chose consist of 2500 biquadratic elements highly concentrated in the melt pool region. A rapid gradation between the liquidus and solidus was achieved with a triangular-element transition layer, thus squandering little computational effort on unwarranted resolution where the fluid mechanics is trivial. The three-dimensional mesh we chose was considerably coarser. Until the necessary physics is built into the two-dimensional model, we cannot justify the cost of the same level of refinement in three dimensions.

Interestingly, predictions at the realistic operating conditions were inaccessible with arbitrary continuation paths. We found it necessary to start at the true Rayleigh number,

2×10^7 , and the true EBeam power and then ramp the production rate up to the desired level. Continuing in Rayleigh number proved impossible, evidently because of a critical point which would require more sophisticated continuation methods to circumvent.

3. RESULTS

All thermophysical properties in the two-dimensional model, e.g. viscosity, density, heat capacity, thermal conductivity, and the coefficient of thermal expansion, are taken for a U6/Nb alloy (Zanner and Bertram 1980). The results we report here are for the crucible ID, 6 inches, depth, 12 inches, wall material and thickness, 0.5 inch copper, and ingot production rate, 150 kg/hr. The axis length of the computational domain was terminated at 12 inches because at that point the ingot had cooled to the temperature of the cooling water.

Figure 2 shows the isotherms (left) and melt pool streamlines (right) calculated with the two-dimensional model. The liquidus and solidus isotherms are indicated in black. The E-Beam-induced heat flux is ramped linearly from 0.01 kW/cm² at the outer edge of the inlet stream (upper left of each figure) to 0.28 kW/cm² at the edge of the crucible. The pattern of streamlines shows the molten metal entering at the top left and driving a counterclockwise recirculation. Locally high surface tension in the cooler region near the crucible wall elongates and strengthens this recirculation. Thermal expansion (buoyancy) drives a counter-rotating recirculation on the right side of the melt pool. The extent and strength of both recirculations can be manipulated with the EBeam power and flux distribution. We believe this effect will be critical in controlling the microstructure of the ingot.

The off-axis feed stream makes the real process three-dimensional. Figure 3 summarizes our progress towards understanding the full three-dimensional momentum and heat transfer process. The EBeam-induced heat flux is spatially uniform, except where the inlet stream shades the surface. The flux is substantially larger (0.4 kW/cm²) in this case. Shown are the isotherms on the inner surface of the crucible (right), the speed contours on a cross-section near the top of the crucible (left), and the path taken by a particle introduced at the inlet (middle). The speed contours show that the inertial cell and the buoyancy cell in the two-dimensional case are actually part of a toroidal recirculation ringing the crucible. The inflow stream clearly broadens this recirculation in its vicinity (see speed contours at left of Figure 3). This asymmetry forces motion to precess the crucible axis, as the particle paths elucidate. The residence time of the particle from the inflow to the point at which it solidifies is about 0.87 s.

The goal of this research is to produce ingots with acceptable homogeneity. The macrosegregation patterns found in ingots produced by almost any remelting process, including the one under study here, are often the factors which limit ingot size (Ridder et al. 1980). The goal here is to develop a predictive tool for analyzing these patterns from computed velocity and temperature fields. We are careful to keep in mind that the real physical phenomena controlling these patterns are much more complicated than we are presently treating them. In fact, computing local average composition C_{Savg} really requires simultaneous solution for flow, thermal, and composition fields. This task is computationally intensive because of the convection-dominated species transport, which to capture would require meshes so dense as to be impractical. Instead we consider the decoupled problem.

We are employing the celebrated Flemings-Mehrabian equation, otherwise known as the "solute-redistribution" equation, to predict compositional changes (Flemings et al. 1968). Combining this equation with that which defines average composition in the mushy zone

(cf. Ridder et al. 1980) and integrating gives an expression for the $\Delta C = C_{\text{Savg}} - C_0$. Here C_{Savg} is the local average composition in both phases and C_0 is the nominal composition of the material, i.e., 6 wt %.

Figure 4 shows ΔC (wt. percent) corresponding to the operating conditions in Figure 2, except for the EBeam flux pattern. Results are shown for two cases. Of course ΔC has meaning only within the mushy zone. For now we have assumed that at some temperature between the liquidus and solidus the mushy fluid is taken as immobile. We have chosen that isotherm at 1550 K (wt. fraction solid 0.2), which is between the liquidus, 1605 K, and solidus, 1400 K. It is that point at which the segregation pattern is set. Although this temperature is somewhat arbitrary, it is noteworthy that the pattern of segregation is quite sensitive to the EBeam flux pattern. In one case the flux pattern is applied uniformly from the edge of the inlet stream to the edge of the crucible, with the flux level being 0.14 kW/cm². In the other case the total power input is the same, but the level is ramped linearly, being low at the edge of the inlet stream and high at the edge of the crucible.

Clearly the flow field and heat transfer field have an effect on the segregation pattern, based on the sensitivity illustrated in Fig. 4. The segregation pattern at the immobilization isotherm appears somewhat smoother in the case for which the EBeam energy is applied uniformly. If the electron gun were programmed to sweep more towards the crucible wall (second case illustrated) the compositional variations would be larger. In either case, based on this simplified analysis and the assumption that the segregation is set at 1550 K, negative segregation would generally be observed in the center of the ingot, and positive near the edges away from the entry region of the feed stream. This qualitatively agrees with the experiments of Zanner and Bertram (1980) with the closely related VAR process, as described above.

4. SUMMARY

In two dimensions it is found that an inertially-driven recirculation in the melt pool interacts with a counter-rotating, buoyancy-driven recirculation, and that both recirculations influence heavily the shape of the solidification front. In three dimensions there is actually a toroidal vortex around which motion precesses.

Our modeling efforts have and will continue to pay off on several fronts: (1) we now understand the role of fluid mechanics in controlling the shape and location of the solidification front; (2) we can learn how to control the flow in the melt pool with the E-beam dwell pattern; and (3) we have a means of probing the sensitivity of the solidification to other operating and design parameters. We believe the tools required to solve the optimization problem (achieve the least segregation) will be in place if this simplified theory for macrosegregation can be validated experimentally. At that point, parameters controlling the EBeam flux distribution can be varied systematically, and the best flux distribution can be predicted, i.e., the distribution that will keep the macrosegregation in the ingot as uniform as possible.

4. REFERENCES

Flemings, M. C., Mehrabian, M. S., and Nereo, G. E., *Trans. TMS-AIME*, **242**, 50-55 (1968).

Ridder, S. D., Mehrabian, R., and Kou, S., "A review of our present understanding of macrosegregation in axi-symmetric ingots", in Modeling of Casting and Welding Processes, H. D. Brody and D. Apelian, eds., The Metallurgical Society of AIME, 261-284 (1980).

Zanner, F. J., and Bertram, L. A., 'Computational and Experimental Analysis of a U-6w/oNb Vacuum Consumable Arc Remelted Ingot," Sandia National Laboratories Technical Report, SAND80-1156, 1980.

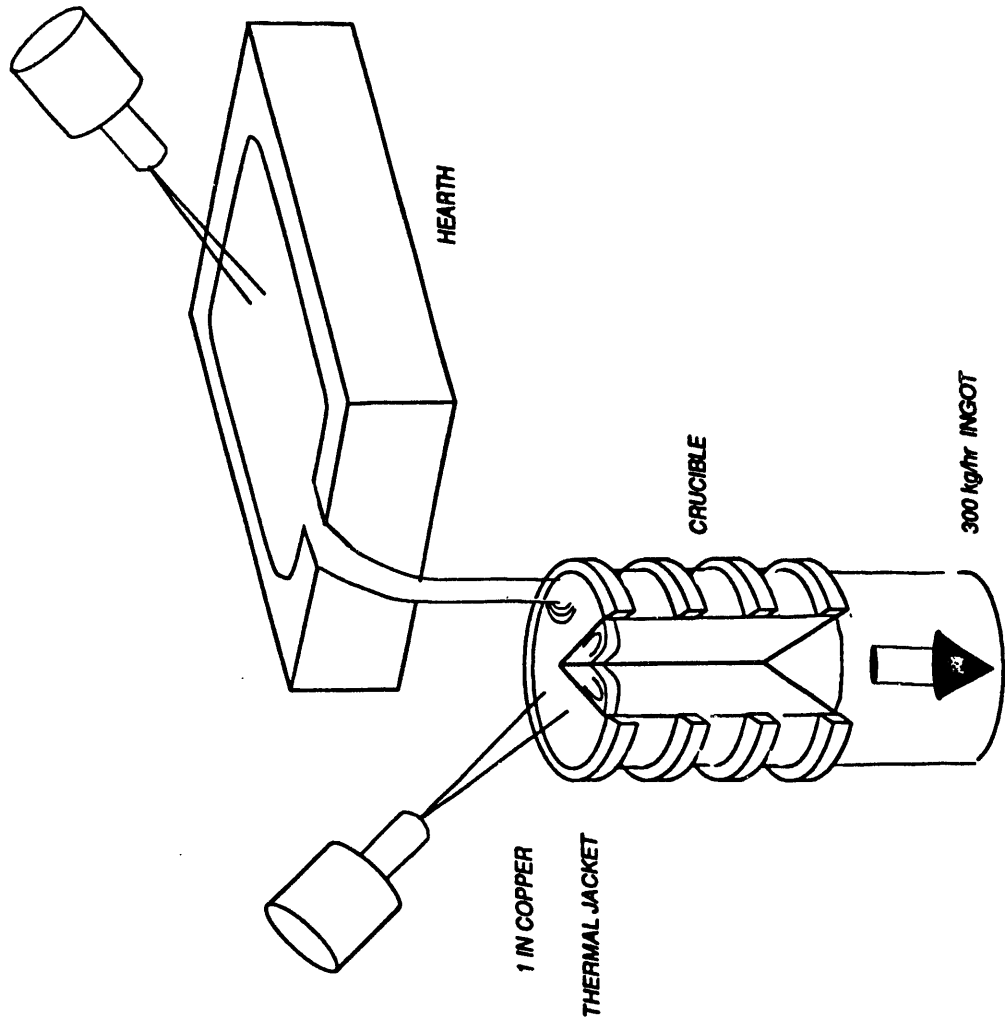


Figure 1: Schematic of the EBeam process.

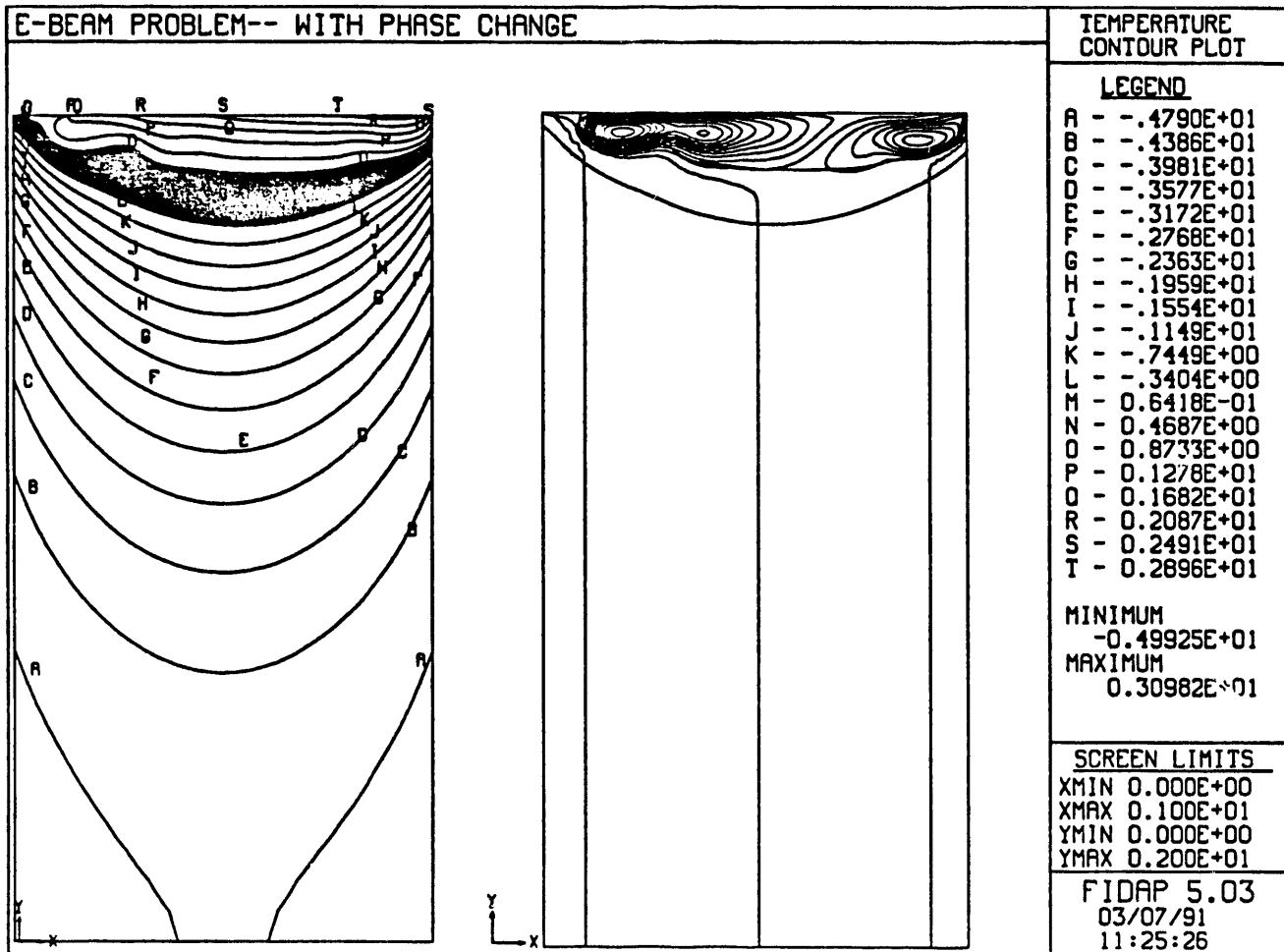


Figure 2: Results from the two-dimensional simulations. The dark region spanning the crucible denotes the mushy zone. The left side shows isotherms corresponding to the scale on the right (one dimensionless temperature unit corresponds to 205 K and zero is the solidus temperature, 1400 K); the right side shows the pattern of streamlines in the melt pool region. The liquid enters at the upper left.

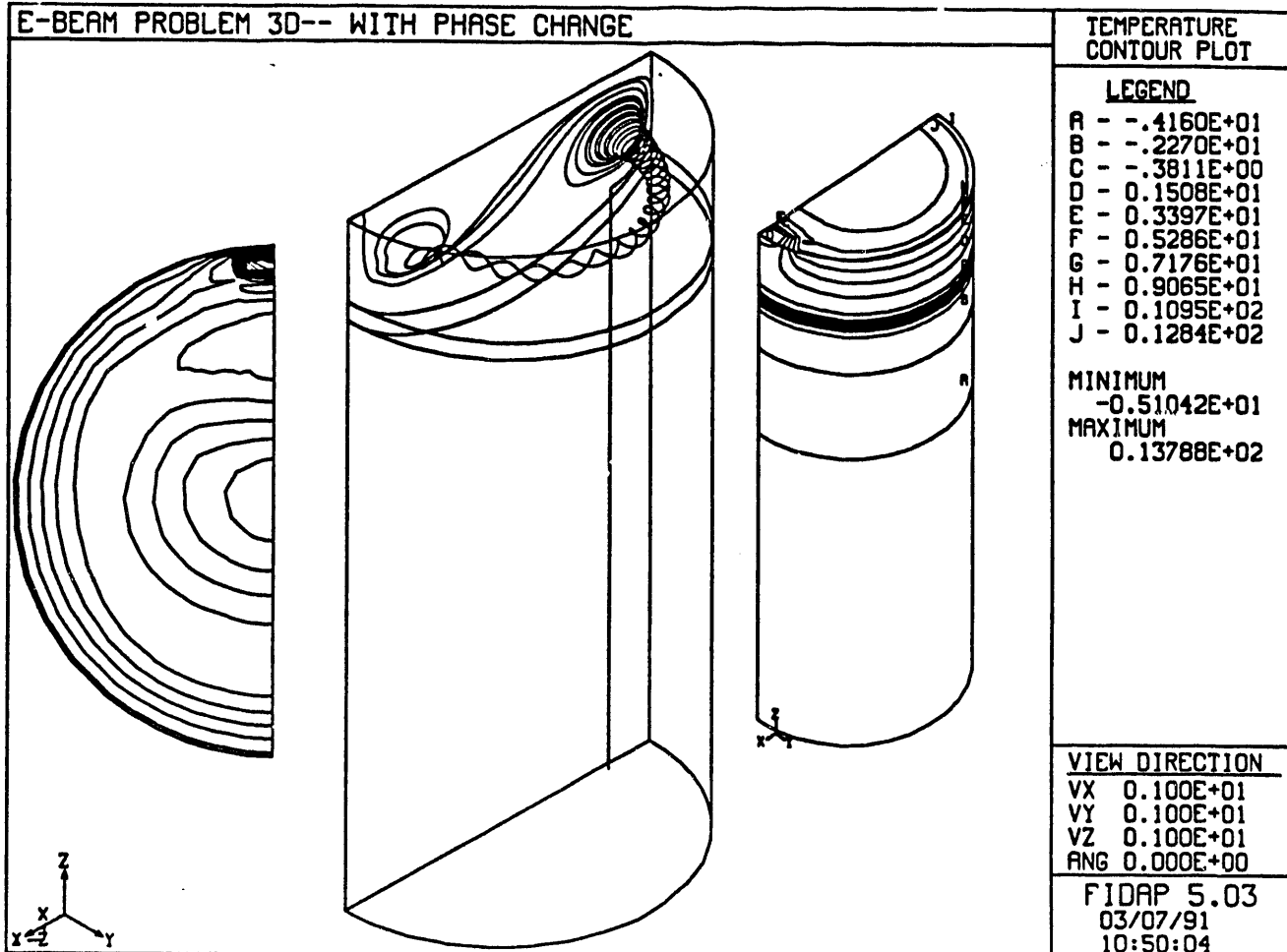


Figure 3: Results from the three-dimensional simulations. Shown are the isotherms (right) corresponding to the scale on the right (one dimensionless temperature unit corresponds to 205 K and zero is the solidus temperature, 1400 K), particle pathlines emanating from the inlet stream (middle), and contours of constant speed (left).

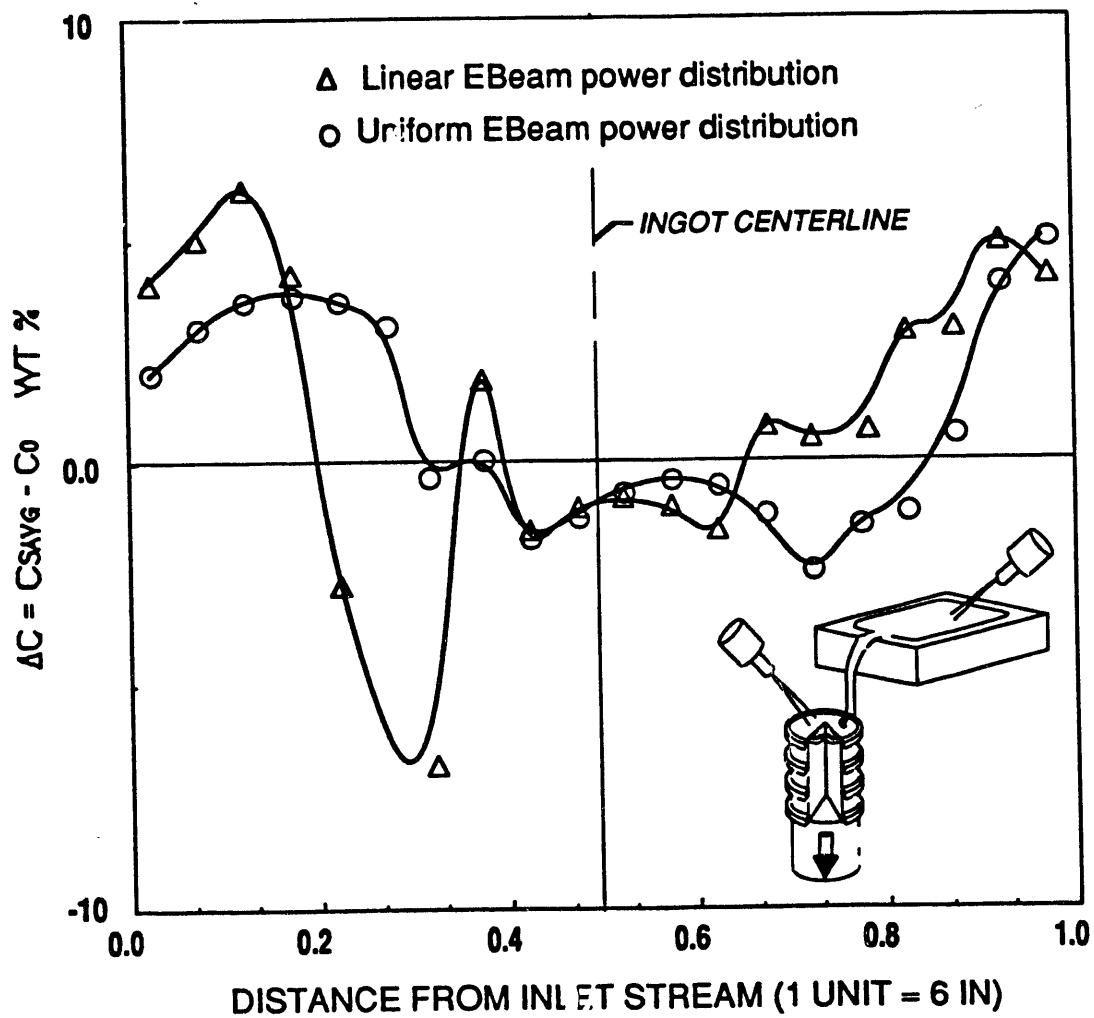


Figure 4: Macrosegregation profiles across two-dimensional ingots. All operating conditions are the same except the EBeam power distribution. The "linear distribution" corresponds to a flux pattern that varies from 0.01 kw/cm^2 at the inlet stream to 0.28 kw/cm^2 at the far edge. The uniform distribution corresponds to a flux that is applied uniformly at 0.14 kw/cm^2 over the same area.

END

DATE
FILMED

12/19/91

